
SUSCEPTIBILITY OF CONTINUAL LEARNING AGAINST ADVERSARIAL ATTACKS

A PREPRINT

Hikmat Khan

Department of Computer Science
COMSATS University Islamabad
Islamabad, Pakistan
hikmat.khan179@gmail.com

Pir Masoom Shah

Department of Computer Science
Bacha Khan University
Charsadda, KPK, Pakistan
pirmasoomshah@bkuc.edu.pk

Syed Farhan Alam Zaidi

Department of Computer Science and Engineering
Chung-Ang University
Seoul, South Korea
syedfarhanalam1993@gmail.com

Saif ul Islam

Department of Computer Science
Institute of Space Technology
Islamabad, Pakistan
saiflu2004@gmail.com

July 14, 2022

ABSTRACT

The recent advances in continual (incremental or lifelong) learning have concentrated on the prevention of forgetting that can lead to catastrophic consequences, but there are two outstanding challenges that must be addressed. The first is the evaluation of the robustness of the proposed methods. The second is ensuring the security of learned tasks remains largely unexplored. This paper presents a comprehensive study of the susceptibility of the continually learned tasks (including both current and previously learned tasks) that are vulnerable to forgetting. Such vulnerability of tasks against adversarial attacks raises profound issues in data integrity and privacy. We consider all three scenarios (i.e, task incremental learning, domain incremental learning and class incremental learning) of continual learning and explore three regularization-based experiments, three replay-based experiments, and one hybrid technique based on the replay and exemplar approach. We examine the robustness of these methods. In particular, we consider cases where we demonstrate that any class belonging to the current or previously learned tasks is prone to misclassification. Our observations, we identify potential limitations in continual learning approaches against adversarial attacks. Our empirical study recommends that the research community consider the robustness of the proposed continual learning approaches and invest extensive efforts in mitigating catastrophic forgetting.

Keywords Continual learning, Vulnerable continual learning, Adversarial attacks, False memory formation

1 Introduction

Deep neural networks have achieved above-human-level accuracy on several tasks, including image classification and recognition, semantic segmentation, bio-medical image analysis, speech recognition, natural language processing, aviation, and playing games [1, 2, 3, 4, 5, 6, 7, 8, 9, 10]. Collective advancement across different scientific disciplines is essential to realizing the long-standing dream of Artificial General Intelligence (AGI) [11]. AGI demands an artificial agent possess two human-like fundamental characteristics, in addition to other intelligent behavior: 1) adaptable and lifelong (or continual) learning capability, i.e., the ability to learn new concepts and adapt to new environments without forgetting previously acquired knowledge, 2) preserved/robust memories, i.e., the ability to safeguard previously acquired abilities [11]. Continuous learning capabilities and historical memory security are integral parts of AGI. In adherence to this, the research community has taken two different approaches. Firstly, continual learning researchers

actively focus on developing algorithms capable of acquiring new concepts consistently without forgetting the prior abilities [12, 13]. Secondly, researchers working in adversarial machine learning have simultaneously demonstrated the vulnerabilities of standard algorithms to adversarial attacks [14, 15].

This paper conducts an empirical study that reveals insight into a series of shortcomings of the existing Task-IL approaches against adversarial attacks. Using Task-IL, we investigate how state-of-the-art continual learning approaches against adversarial attacks rate in terms of security, privacy, and robustness. We consider three regularization-based experiments i.e, Elastic Weight Consolidation (EWC) [16], Elastic Weight Consolidation Online (EWC online) [16] and Synaptic Intelligence (SI) [17]), and three replay based i.e, Learning without Forgetting (Lwf) [18], Deep Generative Replay (DGR) [19] and Deep Generative Replay with Distillation (DGR+Distill) [19]).

2 Related Work

Research on continual learning is active and challenging [20, 21]. It is challenging because of the catastrophic forgetting phenomenon, in which a model experiences rapid performance degradation on past tasks while learning the current task [22, 23]. Section 2.1 reviews the proposed state-of-art approaches to mitigate catastrophic forgetting. In addition to the challenge of mitigating catastrophic forgetting, modern deep learning methods are generally known to have weaker defenses against adversarial attacks. The approaches proposed to highlight the weakness of the deep learning algorithms against adversaries [14, 15]. Section 2.2 briefly sheds light on the weaknesses of the deep learning algorithms against adversaries.

2.1 Continual Learning

We can categorise existing approaches to alleviate catastrophic forgetting into three major categories [24].

Regularization methods: In these approaches, significant changes to the representation learned for previous tasks are prevented, either by regularizing the objective function or directly penalizing the parameters. The method works by constraining weight changes (making them less "flexible") through a loss function to ensure that the learning of new tasks does not alter or has little influence on the performance of previous tasks. Typically, these methods learn to measure the significance of the arch parameters accurately. Examples of such methods include elastic weight consolidation (EWC) [16] and Synaptic Intelligence (SI) [17]. In the EWC method, the crucial parameters have the highest terms in the Fisher information matrix. In contrast, in the SI approach, the parameters' importance is correlated with the loss function: parameters that contribute more to the loss are more important. Generally, in these methods, an additional regularizer term is usually included to ensure that the network parameters remain the same throughout the learning process [25, 26, 27, 28, 29, 30].

Dynamic architectural methods: In these approaches, the objective function remains constant. However, the network capacity (i.e., parameters) exponentially grows in response to new tasks (in different forms such as extra layers, nodes, or modules) upon the arrival of the new tasks. The dynamic architecture commonly works by adding new weights for each task and only allowing those to be tuned. Different subsets of the model parameters are dedicated to each task in parameter isolation methods, in addition to potentially a shared part [31, 32]

Memory-based methods: In these approaches, the prior knowledge is partly retained in order to be utilized later as a kind of rehearsal [33, 34, 35, 36, 37]. The most well-known method is iCaRL [33], which learns in a class-incremental manner by storing samples that are close to the center of each class in fixed memory. Another well-known example of this regime is Averaged Gradient Episodic Memory (A-GEM) [34], which builds a dynamic episodic memory of parameter gradients during the learning process.

2.2 Adversarial Machine Learning

An adversarial attack is the subtle modification of an original input so that the changes are nearly invisible/practically imperceptible to the naked human eye. The modified or altered input is considered an adversary and misclassified when presented to an original classifier, while the unmodified input remains correctly classified [38, 39, 40]. The most frequently modification measures are various euclidean norms (e.g., L_1 , L_2 , L_{inf} etc), which quantify changes at individual pixels [38, 39, 40]. In real life, adversarial attacks can be quite severe, compromise the data's integrity, and can raise difficult questions on safety-critical applications; for instance, an autonomous vehicle may misinterpret a traffic sign, leading to an accident. The most prevalent adversarial attacks called "evasion attack". In evasion attacks, an adversarial example is fed to the network, which is similar to its untempered counterpart but completely confuses the classifier. An adversarial attack occurs in the test phase, but does not modify or affect the original training data.

Black-box attacks vs. White-box attacks: The adversarial attacks can broadly be classified into two categories: *black-box attacks* and *white-box attacks*. The black-box attacks do not require access to the model’s parameters [38]. They only require access to the model’s output. Whereas, white-box attacks require full access to a model’s parameters, hyper-parameters, and architecture details [39, 40].

Target vs. Untarget adversarial attacks: The adversarial attacks can be classified further as *targeted adversarial attacks* and *untargeted adversarial attacks*. In targeted adversarial attacks, the attacker manipulates the source input so that the classifier predicts the input as being a specific target class that differs from the actual input class. While in untargeted adversarial attacks, the attacker aims to craft-fully alter the input such that it is misclassified as any non-target class. In other words, non-targeted attacks are intended to slightly modify the source input in order to misclassify the perturbed input into any class except the truth class. While the targeted attacks are intended to modify the input source in order to misclassify the perturbed input into the target (desired) class except for the truth class.

One-shot vs Iterative adversarial attacks: It is worth noting that the majority of successful attacks use gradient-based techniques, in which the attackers alter the input in the direction of the gradient of the loss function concerning the input. There are two main methods for carrying out such attacks: one-shot attacks, in which the attacker takes a single step in the gradient’s direction, and iterative attacks, in which many steps are performed instead of a single step. The FGSM [38] is a prominent example of one-shot adversarial attacks. PGD and CW are well-known examples of iterative adversarial attacks [39, 40].

In this paper, we examine the vulnerability of continual learning against FGSM (i.e, fast gradient sign method[38]), PGD (i.e, projected Gradient Descent [39]) and CW (i.e, carlini wagner [40]) of continual learning methods (which are categorized in section 2.1 in the three scenarios of continual learning (described in section ??).

Fast Gradient Sign Method (FGSM) [38] is an one shot adversarial attack. Mathematically, it can be described as follows:

$$x^{adv} = x - \varepsilon \cdot \text{sign}(\nabla_x J(x, y_{\text{target}})) \quad (1)$$

where x represents the clean input signal, and x^{adv} represents the perturbed input signal (i.e. the adversarial input). J represents the loss function, and y_{target} represents the targeted label. The ε measure the degree of distortion (i.e., distortion of the input signal) caused by the adversarial attack. The greater the value of ε , the more successful the adversarial attack will be. The ε is the tune-able hyper-parameter.

Projected Gradient Descent (PGD) [39] is an iterative step adversarial attack. Mathematically, it can be described as follows:

$$P_Q(x_0) = \arg \min_{x \in Q} \frac{1}{2} \|x - x_0\|_2^2 \quad (2)$$

In the above equation, x represents the clean input signal, while $x_{[0]}$ represents the starting point in the input space. The Q defines the constraints set (or ball) around the original x . The PGD is an "economic" algorithm if the problem is easy to solve. This isn’t true for general Q and there are lots of constraint sets that are very hard to project onto. If Q is a convex set, the optimization problem has a unique solution. The optimization has a unique solution if Q is a convex set. However, if Q is non-convex, then the solution to $P_Q(x_0)$ may not be unique and gives more than one solution.

Carlini Wagner [40] is an iterative step adversarial attack. Mathematically, it can be described as follows:

$$\text{minimize} \|x - x_0\|^2 + \iota_\Omega \quad (3)$$

$$\iota_\Omega(x) = \begin{cases} 0, & \text{if } \max_{j \neq t} \{g_j(x)\} - g_t(x) \leq 0 \\ +\infty, & \text{otherwise} \end{cases} \quad (4)$$

In the above equation, x represents the clean input signal, while $\iota_\Omega(x)$ represents regularization constraints.

3 Three Scenarios of Continual Learning

Different scenarios for continual learning can be categorised into three main categories [41].

Task incremental learning (Task-IL) is the simplest basic scenario. In this scenario, the task identification is always provided during inference, which enables the model to include the task-specific components (sub-modules in a network

or "multi-headed"), that can be trained along with the task identification information. Typically, the output layer of an architecture is "multi-headed", which means that each task has its own output units, but the rest of the parameters of the network are (possibly) shared between tasks.

Domain incremental learning (Domain-IL) is the second scenario, in which the task identification is unknown at the time of inference. Therefore, models are only required to solve the task but not infer the task identification. Usually, input distribution varies, but output units of the network and basic structure of tasks remain constant.

Class incremental learning (Class-IL) is the third scenario of continuous learning, and it is the most challenging. In sequential order, it presents the continual learning model with a mutually exclusive pair of classes from the same dataset. For instance, if the dataset is composed of ten classes, the dataset will be split into mutually exclusive pairs: [0, 1], [2, 3], [4, 5], [6, 7], and [8, 9].

In this paper, we investigate the robustness of continual learning to adversarial attacks under the three scenarios described above.

4 Methodology

Despite considerable progress in continual learning, we believe that these state-of-the-art algorithms are prone to both catastrophic forgetting and adversarial attacks but that it is also possible to attack any previously learned task and misclassify it. We selected the top-performing algorithms in the respective scenarios of continual learning, see Tables 1, 2 and 3 for details. Specifically, we consider three regularization-based algorithms, namely EWC [16], EWC online [16] and SI [17], three replay-based experiments, namely Lwf [18], DGR [19], and DGR+Distill [19], and one hybrid based on replay and exemplar methods, namely [33]. As for the adversarial attacks, we chose three of the most well-known adversarial attacks: FGSM [38], PGD [39], and CW [40]. We showed experimentally that each learned task of the continual learning methods is vulnerable to three adversarial attacks, i.e., FGSM [38], PGD [39], and CW [40].

4.1 Data Collection

We used standard MNIST dataset for experimentation [42]. The standard MNIST dataset consists of handwritten digits from 0 to 9. It has been used as a standard dataset for training different continual learning algorithms [41]. For instance, SplitMNIST is used to train continual learning models in task incremental learning, while permutedMNIST is used in domain incremental learning, and MNIST is used to train continual learning algorithms in class incremental learning scenarios, where classes (digits) are presented sequentially.

4.2 Evaluation Metric

The models were trained in task incremental learning, domain incremental learning, and continual learning settings. In task incremental settings, we split the MNIST dataset into five tasks consisting of two classes in each task. In domain incremental settings, we split the MNIST dataset into two tasks, each consisting of five classes of MNIST dataset. In the class-incremental setting, we split the MNIST dataset into nine mutually exclusive tasks. The first task consisted of two classes, then one class was added sequentially for each following task. We computed the average accuracy of all the experiments as follows [41]:

$$ACC = \frac{1}{T} \sum_{i=1}^T R_{T,i}, \quad (5)$$

where R stands for the average accuracy, while the i stands for task index.

4.3 Training Protocol

We used the authors' [41] published code to train EWC [16], EWC online [16], SI [17], XDG [43], LwF [18], DGR [19], DGR + distill and ICARL [33] approaches, on MNIST [42] dataset. All hyper-parameter settings were kept the same as in their original papers. Thus, all continual learning methods have achieved similar standard evaluation accuracy as reported in their respective original papers [41]. Each experiment was repeated 20 times with a different seed to achieve a better approximation of the average accuracy, and the mean average accuracy was then calculated with standard deviations over these runs.

4.4 Designing an Adversarial Attacks

We examine the resilience of a previously learned task against three common adversarial attacks, namely FGSM, PGD, and CW [38, 39, 40]. We utilized an open-source python tool called foolbox to create adversarial attacks [44]. We investigate the algorithm’s reliability in each of the three continual learning scenarios for targeted and untargeted attacks. Targeted attacks are the most potent adversarial attacks, while Untargeted attacks are the least powerful ones. An untargeted attack is simply a more efficient (and often less accurate) method of conducting a targeted attack for each target and taking the closest. Our studies demonstrated that all algorithms for continual learning are highly susceptible to adversarial attacks. To summarize, every learned task (either current or historically learning) can be attacked abruptly and misclassified incorrectly into the desired class. Interestingly, we discovered that tasks learned in the past are more prone to misclassification than ones learned lately, resulting in the formation of false memories in an artificial agent. This kind of false memory creation prohibits the artificial agent from being used in real-world scenarios, such as self-driving vehicles.

5 Results and Discussion

We investigate on the robustness of standard continual learning methods against adversarial attacks in general and the security of individual learned tasks in particular. It has been observed that adversarial attacks can be used to attack state-of-the-art continual learning models. Any learned task can be attacked and misclassified easily. It is interesting to note that newly learned tasks are less vulnerable than those historically learned. This underscores the interesting fact that creating false memories of historically learned tasks is easier.

Table 1: The 1st and 2nd columns present the continual learning approaches and the accuracy achieved (averaged across tasks) under standard evaluation settings in task incremental settings. The 3rd, 4th and 5th columns represents the drop in average accuracies under FGSM, PGD and CW adversarial attacks, respectively. The suffice "U" and "T" in columns 3rd, 4th and 5th is to represent the untargeted and targeted adversarial attacks. The drop in average accuracy (i.e, in columns 3rd, 4th and 5th) highlights the success of adversarial attacks and further illustrates that any learned task can be successfully attacked (i.e, misclassified). Each experiment was repeated 20 times with a different seed to achieve a better approximation.

Task IL Setting [41]				
Approach	Task-IL	FGSM [38]	PGD [39]	CW [40]
EWC [16]	98.5%(±0.7)	23.6%(±10.5)-U 32.0%(±10.71)-T	63.1%(±6.5)-U 83.8%(±6.32)-T	98.5%(±0.7)-U 77.6%(±9.38)-T
EWC Online [16]	98.2%(±1.4)	18.9%(±8.0)-U 33.2%(±10.6)-T	59.3%(±8.2)-U 83.0%(±6.69)-T	98.6%(±0.7)-U 84.4%(±6.27)-T
SI [17]	87.8%(±7.5)	23.2%(±6.3)-U 35.8%(±9.9)-T	62.8%(±7.0)-U 78.7%(±7.99)-T	87.8%(±7.5)-U 68.8%(±10.22)-T
XDG [43]	84.7%(±7.5)	32.3%(±5.1)-U 36.9%(±10.01)-T	84.7%(±7.5)-U 66.6%(±9.31)-T	84.7%(±7.5)-U 66.6%(±9.31)-T
LwF [18]	99.4%(±0.2)	14.0%(±8.1)-U 34.8%(±8.12)-T	70.5%(±6.7)-U 91.6%(±4.29)-T	99.4%(±0.2)-U 83.4%(±5.58)-T
DGR [19]	99.5%(±0.2)	53.3%(±9.8)-U 34.2%(±8.17)-T	81.1%(±8.1)-U 92.3%(±4.27)-T	99.5%(±0.2)-U 82.9%(±4.88)-T
DGR + Distill [19]	99.5%(±0.2)	22.5%(±6.1)-U 31.0%(±8.28)-T	65.1%(±6.0)-U 90.5%(±4.88)-T	99.5%(±0.2)-U 84.2%(±4.91)-T

In Tables 1, 2 and 3, we summarized the performance of the continual learning models when attacked by adversarial attacks. The individual class-level vulnerability of the continual learning algorithms under Task-IL can be seen in Figures 1,2,3,5,6,7.

Figure 1 depicts the class-wise vulnerability of the EWC [16] against the FGSM, PGD, and CW [38, 39, 40] adversarial attacks under Task-IL setting of continual learning. Where the first two rows represent the class-wise vulnerability of the EWC against FGSM, and the class-wise vulnerability of the EWC against PGD is shown in the next two rows. The last two rows present the class-wise vulnerability of the EWC against CW. Further, the first subfigure in rows 1,3, and 5 represents the EWC average performance under standard evaluation of continual learning. Similarly, the degradation under untargeted adversarial attacks are presented in the second sub-plots in rows 1, 3, and 5. The following sub-plots show how targeted adversarial attacks degrade average performance. The header of the sub-plots highlights the targeted

Table 2: The 1st and 2nd columns present the continual learning approaches and the accuracy achieved (averaged across tasks) under standard evaluation settings in domain incremental settings. The 3rd and 4th columns represents the drop in average accuracies under FGSM and PGD adversarial attacks, respectively. The suffice "U" and "T" in columns 3rd, 4th and 5th is to represent the untargeted and targeted adversarial attacks. The drop in average accuracy (i.e, in columns 3rd and 4th) highlights the success of adversarial attacks and further illustrates that any learned task can be successfully attacked (i.e, misclassified). Each experiment was repeated 20 times with a different seed to achieve a better approximation.

Domain IL Setting [41]			
Approach	Domain-IL	FGSM[38]	PGD[39]
EWC [16]	78.6%(±4.8)	0.0%(±0.0)-U 19.1%(±2.77)-T	4.4%(±1.7)-U 34.4%(±10.14)-T
EWC Online [16]	78.2%(±5.0)	0.0%(±0.0)-U 19.1%(±2.7)-T	4.7%(±1.7)-U 34.8%(±10.22)-T
SI [17]	66.3%(±4.7)	0.1%(±0.1)-U 18.9%(±2.67)-T	16.4%(±3.0)-U 46.4%(±9.02)-T
XDG [43]	67.0%(±5.2)	0.3%(±0.4)-U 18.8%(±2.68)-T	11.5%(±3.7)-U 40.4%(±9.07)-T
LwF [18]	73.6%(±4.9)	0.0%(±0.0)-U 18.3%(±2.77)-T	3.0%(±1.7) 32.6%(±8.39)-T
DGR [19]	96.3%(±0.7)	1.0%(±1.1)-U 13.2%(±4.8)-T	18.8%(±2.9)-U 30.7%(±9.98)-T
DGR + Distill [19]	96.4%(±0.6)	0.9%(±1.2)-U 14.0%(±4.58)-T	9.9%(±1.5)-U 29.2%(±9.12)-T

Table 3: The 1st and 2nd columns present the continual learning approach and the accuracy achieved (averaged across tasks) under standard evaluation settings in class incremental settings. The 3rd, 4th and 5th columns represents the drop in average accuracies under FGSM, PGD and CW adversarial attacks, respectively. The suffice "U" and "T" in columns 3rd, 4th and 5th is to represent the untargeted and targeted adversarial attacks. The drop in average accuracy (i.e, in columns 3rd, 4th and 5th) highlights the success of adversarial attacks and further illustrates that any learned task can be successfully attacked (i.e, misclassified). Each experiment was repeated 20 times with a different seed to achieve a better approximation.

Class IL Setting [41]				
Approach	Class-IL	FGSM[38]	PGD[39]	CW[40]
ICARL [33]	90.4%(±1.0)	0.5%(±0.6)-U 8.8%(±1.67)-T	3.7%(±2.2)-U 27.8%(±8.72)-T	0.1%(±0.0)-U 10.0%(±0.41)-T

labels. Moreover, x-axis of the plots represents the task number while y-axis represents the average accuracy over 10 runs.

Similarly, Figure 2 shows the class-wise vulnerability of the EWC online [16] against the FGSM, PGD, and CW [38, 39, 40] adversarial attacks under Task-IL setting of continual learning. The initial two rows present the class-wise vulnerability of the EWC online against FGSM. The next two rows depict the class-wise vulnerability of the EWC online against PGD, and the last two rows present the class-wise vulnerability of the EWC online against CW. Moreover, the first sub-figure in rows 1, 3, and 5 presents the EWC online average performance under standard evaluation of continual learning. The second sub-plots in rows 1, 3, and 5 present the degradation under untargeted adversarial attacks. The subsequent sub-plots show how targeted adversarial attacks degrade the overall performance. The sub-plots' headers point to the labels that are being targeted. The number on x-axis indicates the task number while the y-axis presents the average accuracy over 10 runs.

The class-wise vulnerability of the SI [17] against the FGSM, PGD, and CW [38, 39, 40] adversarial attacks under Task-IL setting of continual learning is depicted in Figure 3. The first and second row depicts the class-wise vulnerability of the SI against FGSM. Similarly, the third and fourth row shows the class-wise vulnerability of the SI against PGD, and the fifth and sixth row presents the class-wise vulnerability of the SI against CW. The first sub-figure in rows 1, 3, and 5 presents the SI average performance under standard evaluation of continual learning. The degradation under untargeted adversarial attacks is depicted in the second sub-plots in rows 1, 3, and 5. Furthermore, the following sub-plots show the decline in average performance as a result of targeted adversarial attacks. The headers of the

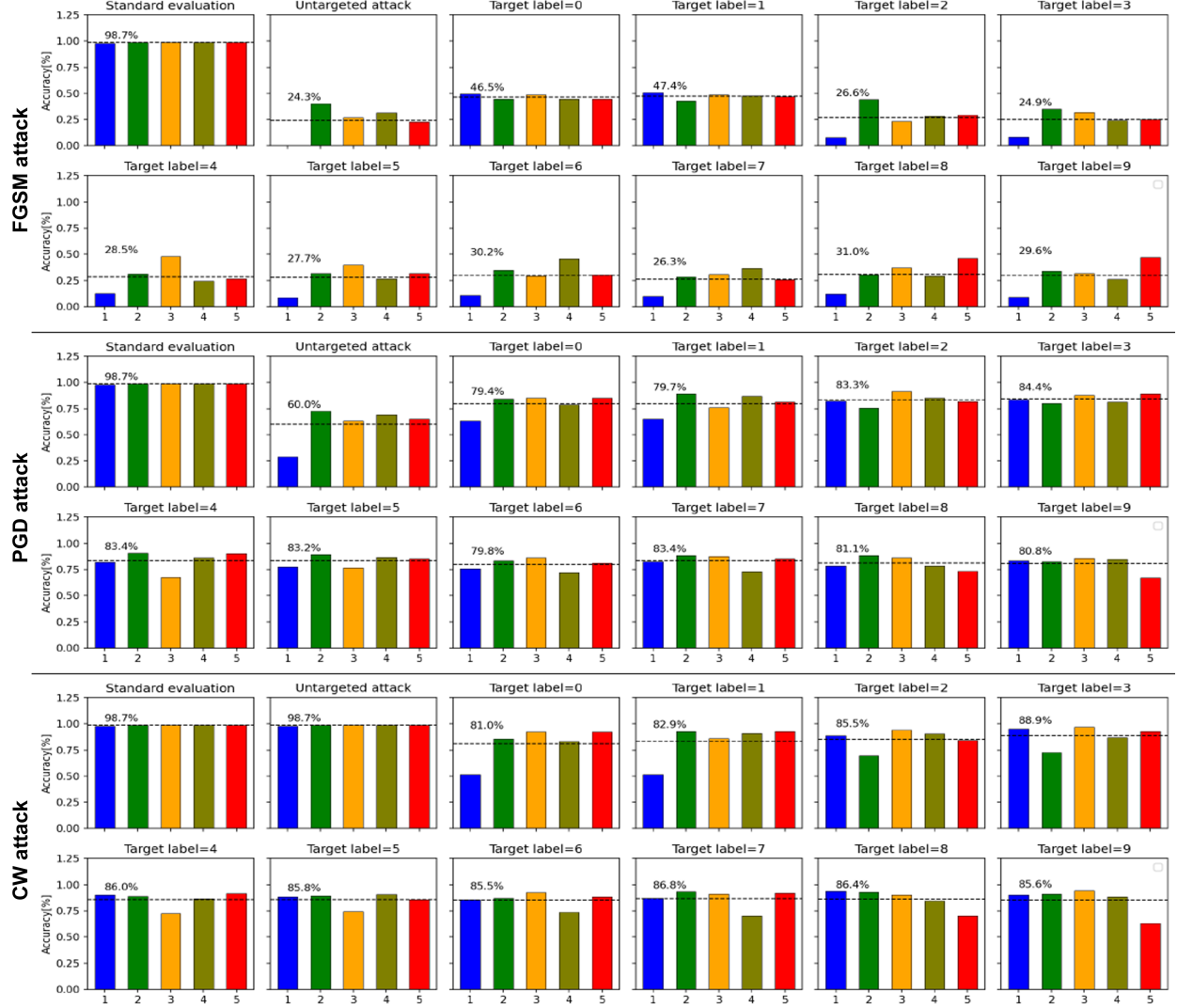


Figure 1: Class-wise vulnerability of the EWC [16] against the FGSM, PGD, and CW [38, 39, 40] adversarial attacks under Task-IL setting of continual learning.

sub-plots bring attention to the targeted labels. The x-axis represents the task number while the y-axis shows the average accuracy over 10 runs.

Figure 4 presents the class-wise vulnerability of the XDG [43] against the FGSM [38] adversarial attacks under Task-IL setting of continual learning. The targeted labels are highlighted in the subplots' headers. The number on x-axis indicates the task number while the y-axis points to the average accuracy over 10 runs.

In addition, Figure 5 shows the class-wise vulnerability of the Lwf [18] against the FGSM, PGD, and CW [38, 39, 40] adversarial attacks under Task-IL setting of continual learning. The initial two rows present the class-wise vulnerability of the Lwf against FGSM. The next two rows depict the class-wise vulnerability of the Lwf against PGD, and the final two rows present the class-wise vulnerability of the Lwf against CW. The first sub-figure in rows 1, 3, and 5 shows the Lwf average performance under standard evaluation of continual learning. Subsequently, the second sub-plots in rows 1, 3, and 5 present the degradation under untargted adversarial attacks. The following sub-plots show the way the average performance deteriorates as a result of targeted adversarial attacks. The sub-plots' headings highlight the targeted labels. The x-axis shows the task number while the y-axis depicts the average accuracy over 10 runs.

Figure 6 presents the class-wise vulnerability of the DGR [19] against the FGSM, PGD, and CW [38, 39, 40] adversarial attacks under Task-IL setting of continual learning. The first and second row depicts the class-wise vulnerability of the DGR against FGSM. Similarly, the third and fourth row shows the class-wise vulnerability of the DGR against PGD,

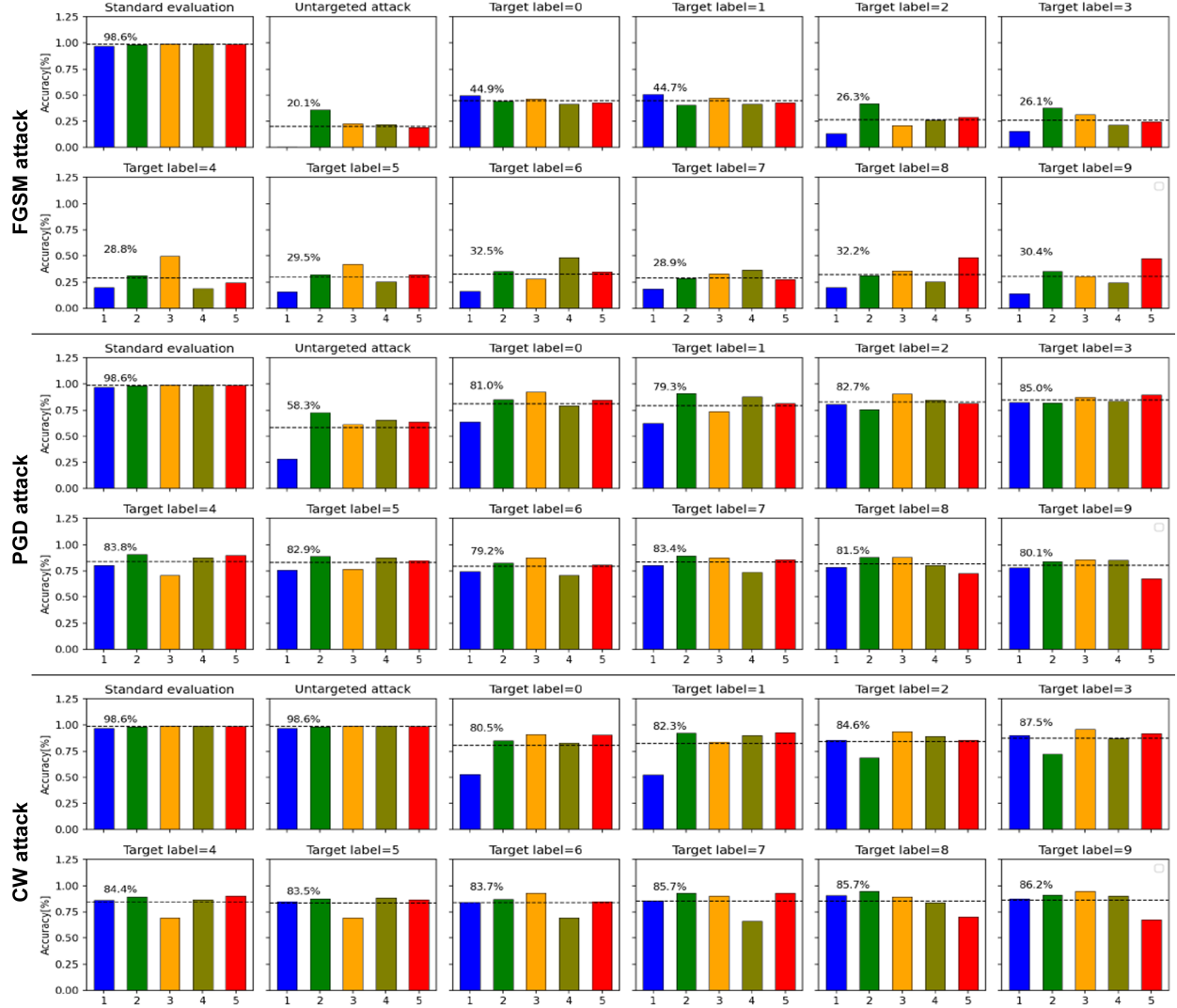


Figure 2: class-wise vulnerability of the EWC online [16] against the FGSM, PGD, and CW [38, 39, 40] adversarial attacks under Task-IL setting of continual learning.

and the fifth and sixth row presents the class-wise vulnerability of the DGR against CW. The first sub-figure in rows 1, 3, and 5 depicts the Lwf average performance under standard evaluation of continual learning. The degradation under untargeted adversarial attacks is depicted in the second sub-plots in rows 1, 3, and 5. The following sub-plots show the decline in average performance as a result of targeted adversarial attacks. The sub-plots' headers draw attention to the targeted labels. The number on x-axis represents the task number while the y-axis shows the average accuracy over 10 runs.

Furthermore, Figure 7 illustrates the class-wise vulnerability of the DGR+Distill [19] against the FGSM, PGD, and CW [38, 39, 40] adversarial attacks under Task-IL setting of continual learning. The top two rows present the class-wise vulnerability of the DGR+Distill against FGSM. The following two rows show the class-wise vulnerability of the DGR+Distill against PGD, and the bottom two rows depict the class-wise vulnerability of the DGR+Distill against CW. The first sub-figure in rows 1, 3, and 5 presents the Lwf average performance under standard evaluation of continual learning. The second sub-plots in rows 1, 3, and 5 indicate the degradation caused by untargeted adversarial attacks. The following sub-plots show how targeted adversarial attacks degrade average performance. The sub-plots' headers point to the labels that are being targeted. Moreover, x-axis of the plots represents the task number while y-axis represents the average accuracy over 10 runs.

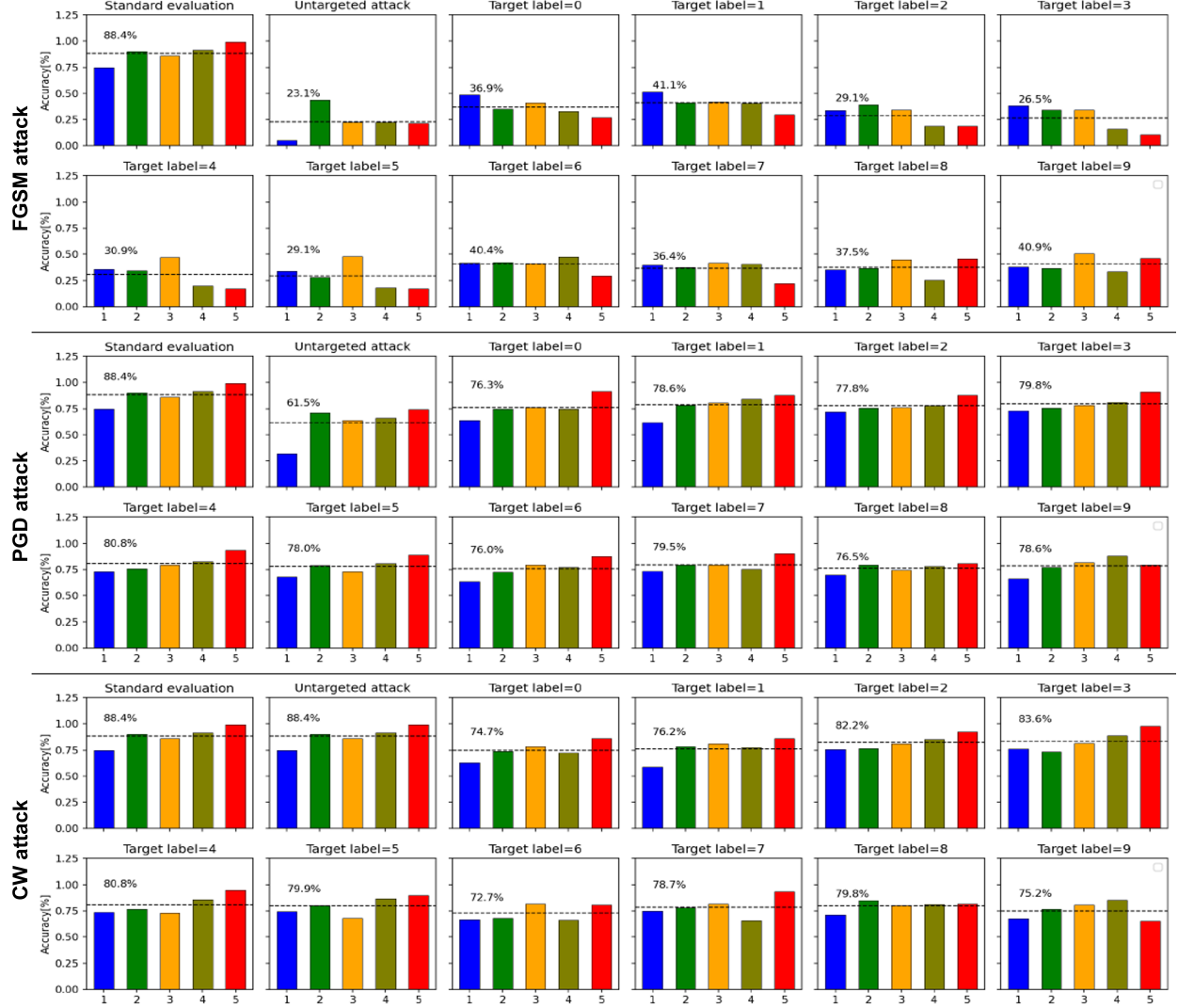


Figure 3: Class-wise vulnerability of the SI [17] against the FGSM, PGD, and CW [38, 39, 40] adversarial attacks under Task-IL setting of continual learning.

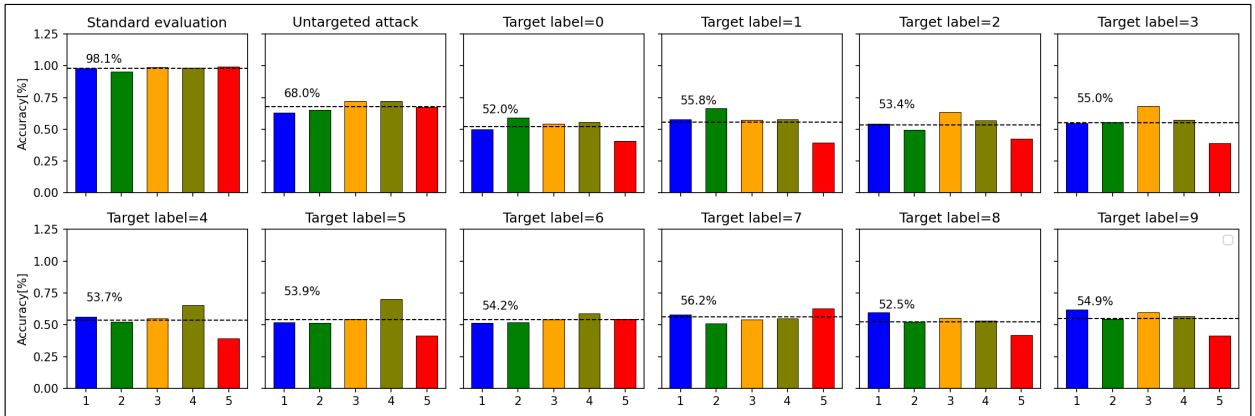


Figure 4: Class-wise vulnerability of the XDG [43] against the FGSM [38] adversarial attacks under Task-IL setting of continual learning.

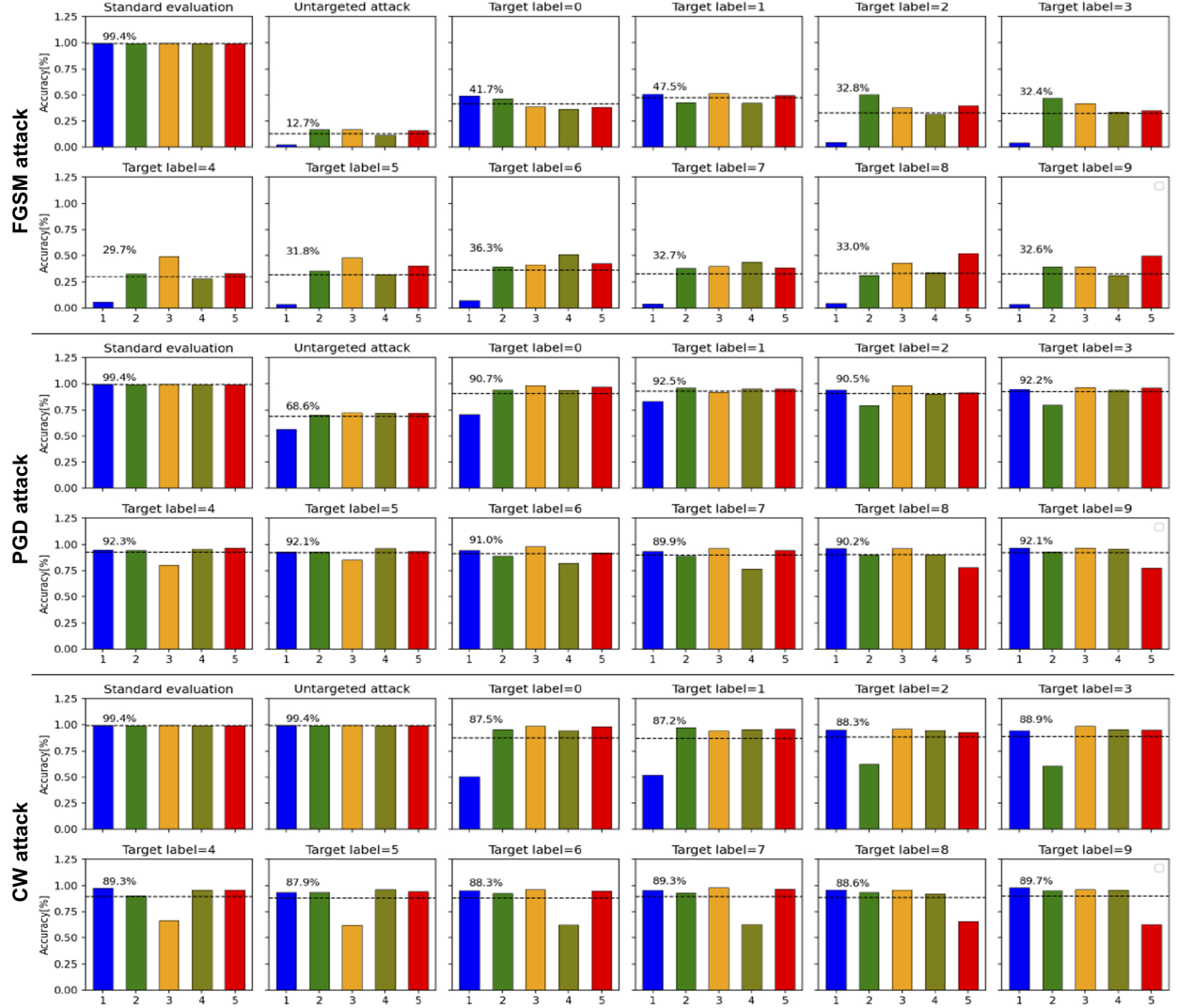


Figure 5: Presents class-wise vulnerability of the Lwf [18] against the FGSM, PGD, and CW [38, 39, 40] adversarial attacks under Task-IL setting of continual learning.

Figure 8 depicts the class-wise vulnerability of the EWC [16] against the FGSM [38] adversarial attacks under Domain-IL setting of continual learning. The first row depicts the class-wise vulnerability of the EWC against FGSM, and the second row presents the class-wise vulnerability of the ICARL against PGD. The first sub-figure in rows 1 and 2 shows the average performance of EWC under standard evaluation of continual learning. The degradation under untargeted adversarial attacks is depicted in the second sub-plots in rows 1 and 2. The subsequent sub-plots show how targeted adversarial attacks degrade the overall performance. The header of the sub-plots highlights the targeted labels. The number on x-axis indicates the task number while the y-axis presents the average accuracy over 10 runs. The horizontal bar represents the average accuracy obtained across two tasks.

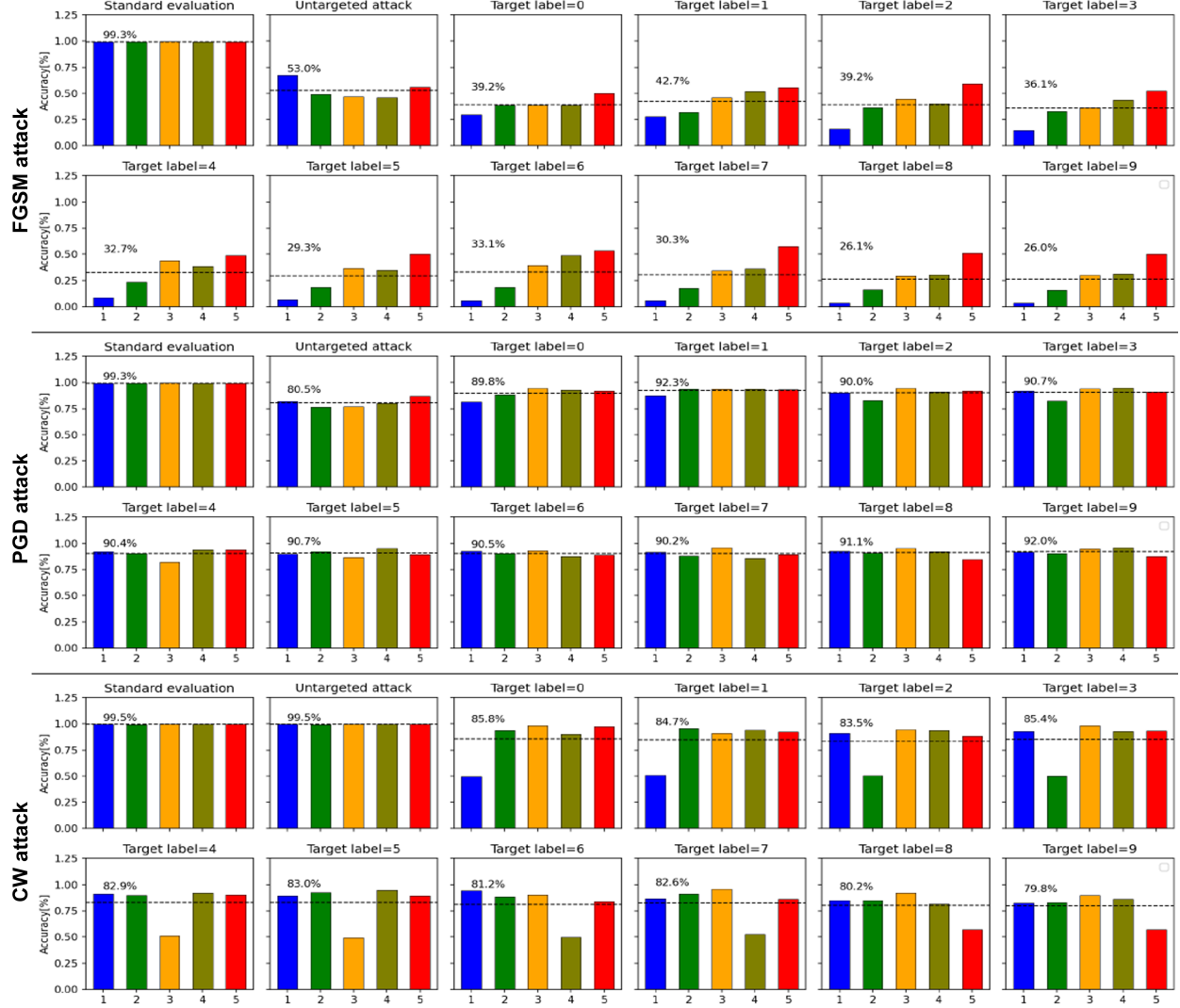


Figure 6: Presents class-wise vulnerability of the DGR [19] against the FGSM, PGD, and CW [38, 39, 40] adversarial attacks under Task-IL setting of continual learning.



Figure 8: Class-wise vulnerability of the EWC [16] against the FGSM and PGD [38, 39] adversarial attacks under Domain-IL setting of continual learning.

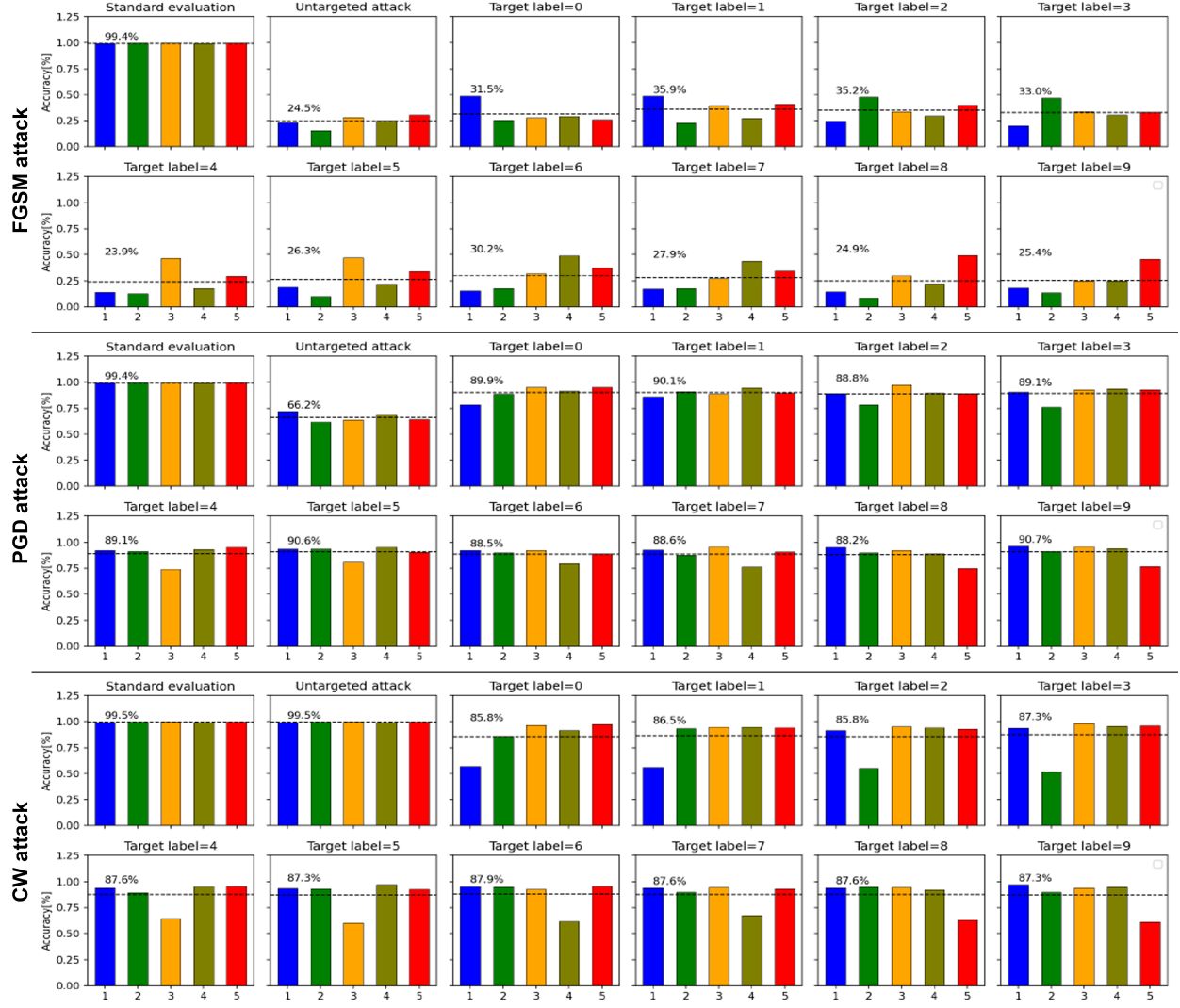


Figure 7: Presents class-wise vulnerability of the DGR+Distill [19] against the FGSM, PGD, and CW [38, 39, 40] adversarial attacks under Task-IL setting of continual learning.

In addition, Figure 9 presents the class-wise vulnerability of the EWC online [16] against the FGSM [38] adversarial attack under Domain-IL setting of continual learning. Initially, the first row shows the class-wise vulnerability of the EWC online against FGSM and then the second row depicts the class-wise vulnerability of the ICARL against PGD. The first sub-figure in rows 1 and 2 presents the average performance of EWC online under standard evaluation of continual learning. The second sub-plots in rows 1 and 2 show the degradation caused by untargeted adversarial attacks. The following sub-plots show the way the average performance deteriorates as a result of targeted adversarial attacks. The sub-plots' headings highlight the targeted labels. The x-axis shows the task number while the y-axis depicts the average accuracy over 10 runs. The horizontal bar depicts the average accuracy achieved throughout two tasks.

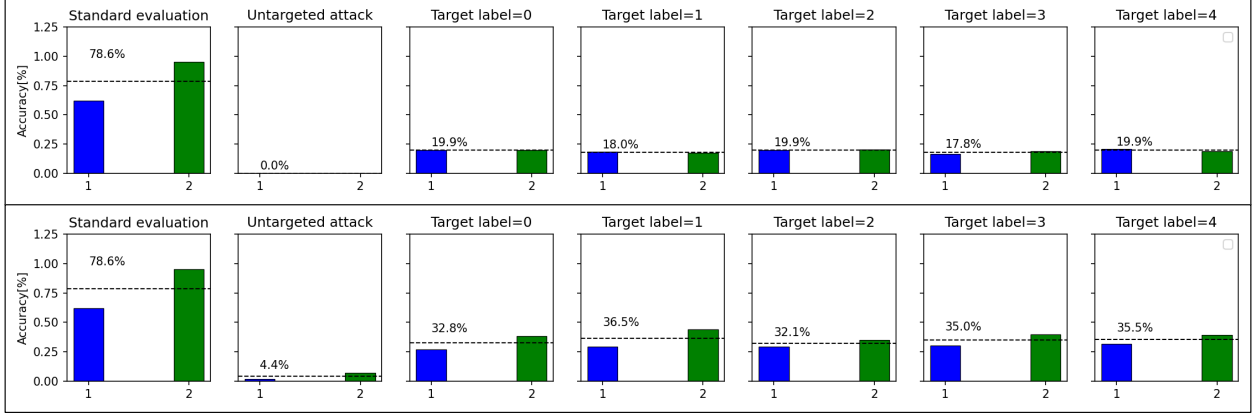


Figure 9: Presents class-wise vulnerability of the EWC online [16] against the FGSM and PGD [38, 39] adversarial attacks under Domain-IL setting of continual learning.

Figure 10 illustrates the class-wise vulnerability of the SI [17] against the FGSM [38] adversarial attacks under Domain-IL setting of continual learning. The first row shows the class-wise vulnerability of the SI against FGSM, and the second row presents the class-wise vulnerability of the SI against PGD. The first sub-figure in rows 1 and 2 depicts the average performance of SI under standard evaluation of continual learning. The second sub-plots in rows 1 and 2 present the degradation under untargeted adversarial attacks. Furthermore, the following sub-plots show the decline in average performance as a result of targeted adversarial attacks. The headers of the sub-plots bring attention to the targeted labels. The x-axis represents the task number while the y-axis shows the average accuracy over 10 runs. The horizontal bar shows the average accuracy of two tasks.

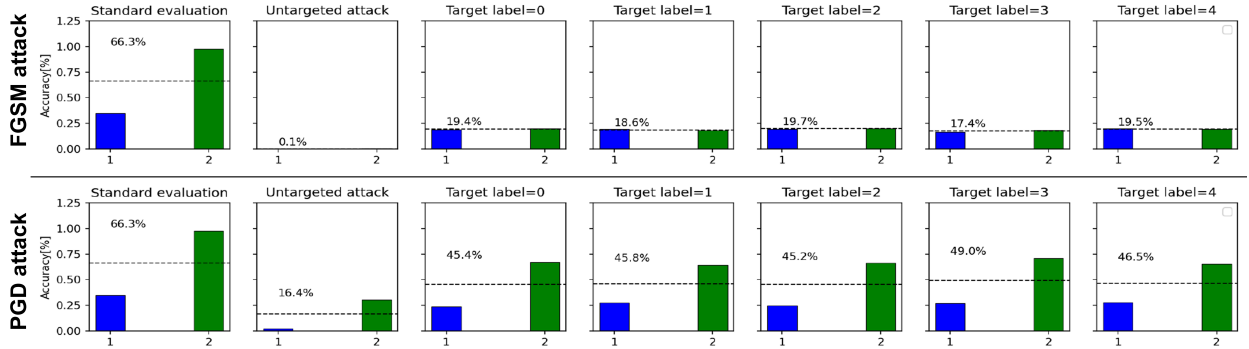


Figure 10: Presents class-wise vulnerability of the SI [17] against the FGSM and PGD [38, 39] adversarial attacks under Domain-IL setting of continual learning.

Similarly, Figure 11 presents the class-wise vulnerability of the XDG [43] against the FGSM [38] adversarial attacks under Domain-IL setting of continual learning. Row 1 depicts the class-wise vulnerability of the XDG against FGSM, and row 2 shows the class-wise vulnerability of the XDG against PGD. The first sub-figure in rows 1 and 2 presents average performance of XDG under standard evaluation of continual learning. The degradation under untargeted adversarial attacks is depicted in the second sub-plots in rows 1 and 2. The following sub-plots show the decline in average performance as a result of targeted adversarial attacks. The targeted labels are highlighted in the sub-plots' headers. The task number appears on the x-axis, while the average accuracy over 10 runs appears on the y-axis. The horizontal bar depicts the average accuracy achieved throughout two tasks.

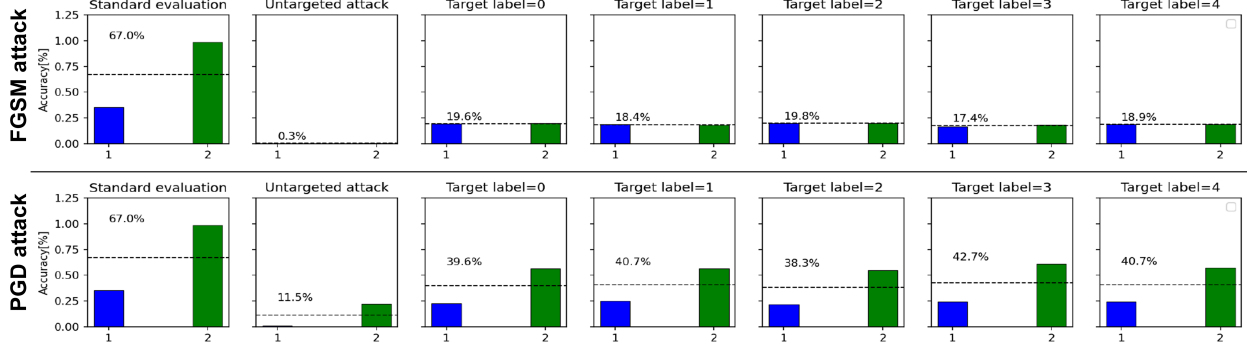


Figure 11: Presents class-wise vulnerability of the XDG [43] against the FGSM and PGD [38, 39] adversarial attacks under Domain-IL setting of continual learning.

Figure 12 depicts the class-wise vulnerability of the DGR [19] against the FGSM [38] adversarial attacks under Domain-IL setting of continual learning. The class-wise vulnerability of the DGR against FGSM is presented in row 1, and the class-wise vulnerability of the DGR against PGD is showed in row 2. The first sub-figure in rows 1 and 2 shows the average performance of DGR under standard evaluation of continual learning. The degradation induced by untargeted adversarial attacks is depicted in the second sub-plots in rows 1 and 2. The following sub-plots indicate how targeted adversarial attacks have lowered the average performance. Headers of the sub-plots highlights the targeted labels. Moreover, x-axis of the plots represents the task number while y-axis represents the average accuracy over 10 runs. The average accuracy of the two tasks is represented by the horizontal bar.

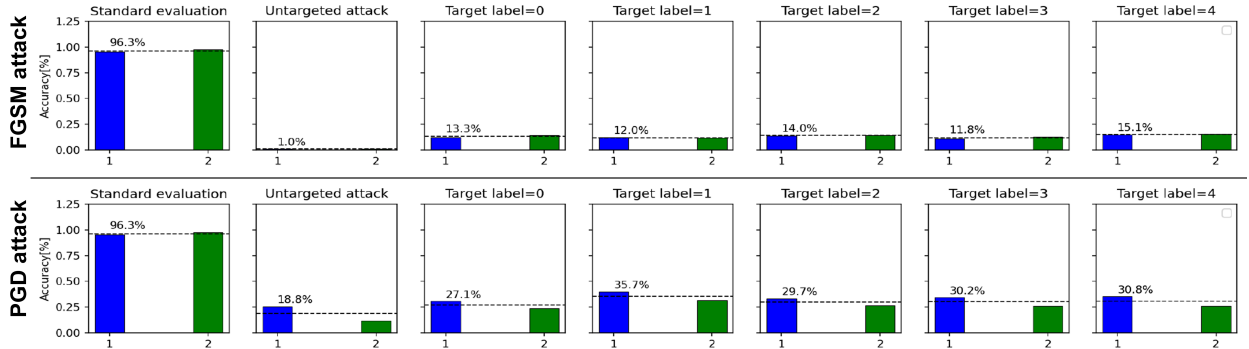


Figure 12: Presents class-wise vulnerability of the DGR [19] against the FGSM and PGD [38, 39] adversarial attacks under Domain-IL setting of continual learning.

Finally, Figure 13 illustrates the class-wise vulnerability of the ICARL [33] against the FGSM, PGD, and CW [38, 39, 40] adversarial attacks under Class-IL setting of continual learning. The first and second rows present the class-wise vulnerability of the ICARL against FGSM. Similarly, the third and fourth rows present the class-wise vulnerability of the ICARL against PGD, and the fifth and sixth rows present the class-wise vulnerability of the ICARL against CW. The first sub-figure in rows 1, 3, and 5 presents the Lwf average performance under standard evaluation of continual learning. In the second sub-plot of rows 1 and 2, the degradation caused by untargeted adversarial attacks is displayed. The sub-plots' headers point to the labels that are being targeted. Moreover, x-axis of the plots represents the task number while y-axis represents the average accuracy over 10 runs.

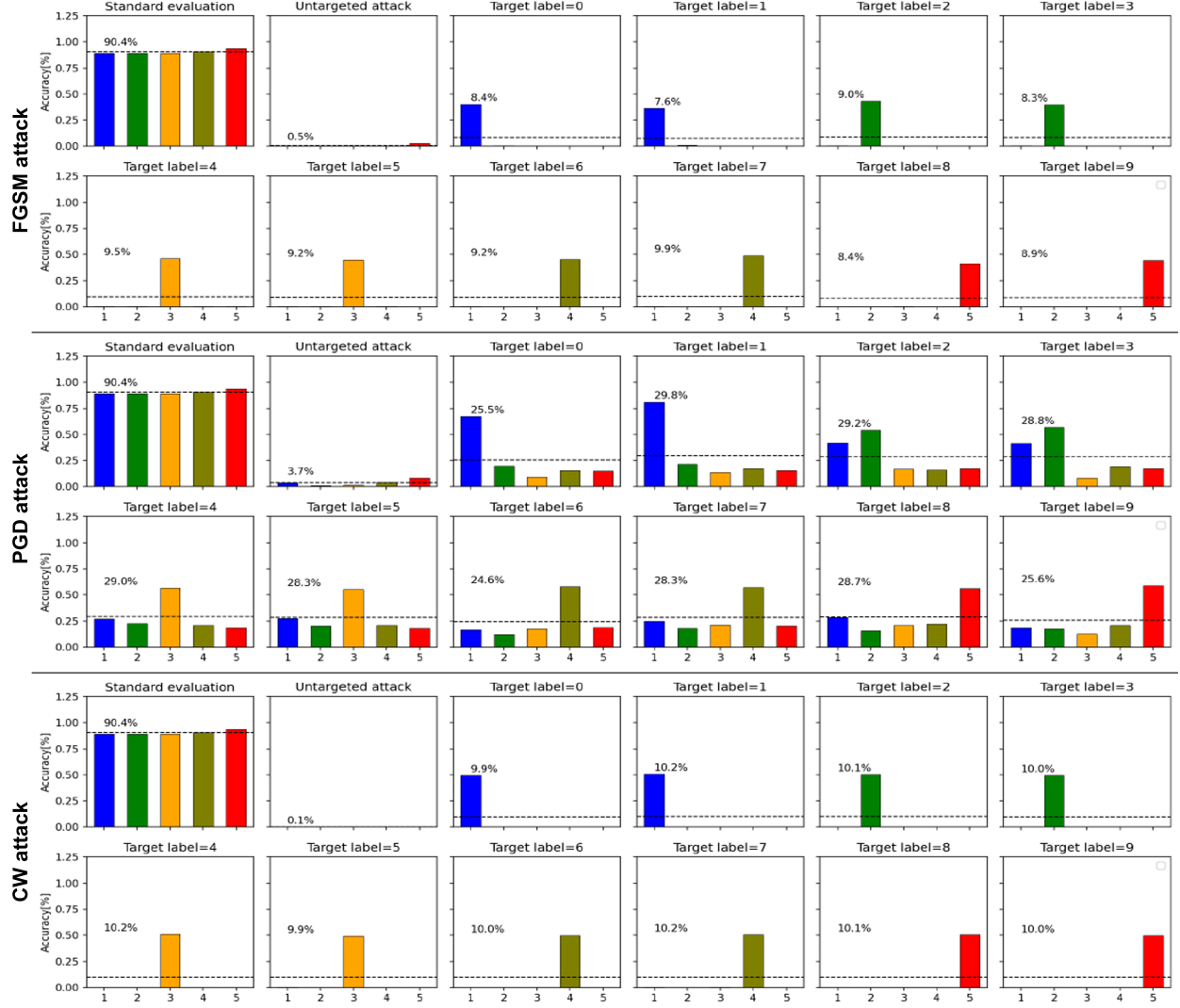


Figure 13: Presents class-wise vulnerability of the ICARL [33] against the FGSM, PGD, and CW [38, 39, 40] adversarial attacks under Class-IL setting of continual learning.

The individual class-level vulnerability of the continual learning algorithms under Domain-IL can be seen in Figures 8,9,10,11 and 12. Similarly, The individual class-level vulnerability of the continual learning algorithms under Class-IL can be seen in Figures 13.

Adversarial Attack in Task-IL settings Figures 1, 2, 3, 5, 6 and 7 present the class-class and average drops in accuracy for EWC, EWC online, SI, Lwf, DGR and DGR+Distill methods against FGSM, PGD, and CW adversarial attacks, respectively.

Adversarial Attack in Domain-IL settings Figure 8, 9, 10, 11 and 12 present the class-wise and average drops in accuracy for EWC, EWC online, SI, XDG and DGR method against FGSM and PGD adversarial attacks trained in domain incremental setting.

Adversarial Attack in Class-IL settings Figure 13 presents the class-wise and average drops in accuracy for ICARL method against FGSM, PGD, and CW adversarial attacks trained in class incremental setting. Our empirical results demonstrate the need to initiate a new research direction, such as robust continual learning (just like robust machine learning or trustworthy machine learning) with a core focus on developing techniques that not only prevent catastrophic forgetting but also provide guarantees to not allowing any compromising impact on the security of the historically learned tasks. Because such a weaker defense against the adversarial examples limits the applicability of the continual learning-based solutions and in fact, entirely defeats its purpose of continual learning algorithm or artificial agent.

For instance, an adversary, which can slightly modify a malware file and become classified as benign in an old or current task, has entirely defeated the malware classifier. The continual learning algorithms should not only prevent catastrophic forgetting but also offers sound robustness so that they could easily be deployed in security-critical real-world environments. As we have seen that almost all the state-of-the-art continual learning methods suffer severely against adversarial attacks. Therefore, based on our observations, we suggest that besides evaluating the model based on less catastrophic forgetting, the continual learning research community should also include additional metrics that measure the robustness of the proposed methods to ensure the model’s security. Finally, our observations indicate that the algorithms’ tendency to enable false memory formation is exacerbated by the ease with which learning activities may be misclassified. Our observations also indicate that the algorithms’ tendency to produce false memories is caused by the ease with which learning activities may be classified incorrectly.

6 Conclusion

We have demonstrated that any class belonging to current or previously learned tasks can be misclassified by simply creating an adversary example of a desire class. We found that adversarial attacks were successful in all three scenarios: task-incremental learning, domain-incremental learning, and class-incremental learning for state-of-the-art continual learning methods, including EWC, EWC online, SI, XDG, LwF, DGR, DGR+Distill, and iCARL. We demonstrate empirically that continual learning techniques are more vulnerable to adversarial attacks. We strongly recommend that the research community invest significant effort to enhance the robustness of continuous learning approaches to prevent such situations from occurring.

7 Future Research Directions

Our understanding of neural network optimization has evolved significantly in recent years, and we expect this trend to continue. We anticipate that future work will continue to leverage the geometry of the objective landscape for more accurate and reliable neural networks. We suggest to perform the adversarial training for each task during the training phase to better understand the robustness of each model along with standard supervised learning. We hope that the adversarial training will make the continual learning models to resist the adversarial attacks and prevent the risk of false memory formation in historically learned tasks. However, there might be other confounding acute (e.g., Backdoor attacks on the previous tasks), which could further shed light on the robustness of the previous tasks for these approaches. Thus, we call for more theoretical research to further their role in demystifying the security of continual learning. Interestingly, this article empirically observes that continual learning techniques proved to be more vulnerable against adversarial attacks.

References

- [1] Lei Cai, Jingyang Gao, and Di Zhao. A review of the application of deep learning in medical image classification and segmentation. *Annals of translational medicine*, 8(11), 2020.
- [2] Daniel W Otter, Julian R Medina, and Jugal K Kalita. A survey of the usages of deep learning for natural language processing. *IEEE transactions on neural networks and learning systems*, 32(2):604–624, 2020.
- [3] Jiwoong J Jeong, Amara Tariq, Tobiloba Adejumo, Hari Trivedi, Judy W Gichoya, and Imon Banerjee. Systematic review of generative adversarial networks (gans) for medical image classification and segmentation. *Journal of Digital Imaging*, pages 1–16, 2022.
- [4] Babita Pandey, Devendra Kumar Pandey, Brijendra Pratap Mishra, and Wasiur Rhmann. A comprehensive survey of deep learning in the field of medical imaging and medical natural language processing: Challenges and research directions. *Journal of King Saud University-Computer and Information Sciences*, 2021.
- [5] Ashima Yadav and Dinesh Kumar Vishwakarma. Sentiment analysis using deep learning architectures: a review. *Artificial Intelligence Review*, 53(6):4335–4385, 2020.
- [6] Ngan Le, Vidhiwar Singh Rathour, Kashu Yamazaki, Khoa Luu, and Marios Savvides. Deep reinforcement learning in computer vision: a comprehensive survey. *Artificial Intelligence Review*, pages 1–87, 2021.
- [7] Khan Hikmat, Pir Masoom Shah, Munam Ali Shah, Saif ul Islam, and Joel JPC Rodrigues. Cascading handcrafted features and convolutional neural network for iot-enabled brain tumor segmentation. *Computer Communications*, 153:196–207, 2020.

- [8] Khan Hikmat, Rasool Ghulam, Bouaynaya Nidhal, C, and Johnson Charles C. Rotorcraft flight information inference from cockpit videos using deep learning. *American Helicopter Society 75th Annual Forum, Philadelphia, Pennsylvania, USA*, May 2019.
- [9] Khan Hikmat, Rasool Ghulam, Bouaynaya Nidhal, C, , Travis Tyler, Thompson Lacey, and Johnson Charles C. Explainable ai: Rotorcraft attitude prediction. *Vertical Flight Society's 76th Annual Forum and Technology Display, Virginia Beach, Virginia, USA*, Oct 2020.
- [10] Khan Hikmat, Rasool Ghulam, Bouaynaya Nidhal, C, , Travis Tyler, Thompson Lacey, and Johnson Charles C. Deep ensemble for rotorcraft attitude prediction. *Vertical Flight Society's 77th Annual Forum and Technology Display, Palm Beach, Florida, USA*, May 2021.
- [11] Xiangming Zeng and Liangqu Long. Introduction to artificial intelligence. In *Beginning Deep Learning with TensorFlow*, pages 1–45. Springer, 2022.
- [12] German I Parisi, Ronald Kemker, Jose L Part, Christopher Kanan, and Stefan Wermter. Continual lifelong learning with neural networks: A review. *Neural Networks*, 113:54–71, 2019.
- [13] Matthias Delange, Rahaf Aljundi, Marc Masana, Sarah Parisot, Xu Jia, Ales Leonardis, Greg Slabaugh, and Tinne Tuytelaars. A continual learning survey: Defying forgetting in classification tasks. *IEEE Transactions on Pattern Analysis and Machine Intelligence*, 2021.
- [14] Xianmin Wang, Jing Li, Xiaohui Kuang, Yu-an Tan, and Jin Li. The security of machine learning in an adversarial setting: A survey. *Journal of Parallel and Distributed Computing*, 130:12–23, 2019.
- [15] Anirban Chakraborty, Manaar Alam, Vishal Dey, Anupam Chattopadhyay, and Debdeep Mukhopadhyay. Adversarial attacks and defences: A survey. *arXiv preprint arXiv:1810.00069*, 2018.
- [16] James Kirkpatrick, Razvan Pascanu, Neil Rabinowitz, Joel Veness, Guillaume Desjardins, Andrei A Rusu, Kieran Milan, John Quan, Tiago Ramalho, Agnieszka Grabska-Barwinska, et al. Overcoming catastrophic forgetting in neural networks. *Proceedings of the national academy of sciences*, 114(13):3521–3526, 2017.
- [17] Friedemann Zenke, Ben Poole, and Surya Ganguli. Continual learning through synaptic intelligence. *Proceedings of machine learning research*, 70:3987, 2017.
- [18] Zhizhong Li and Derek Hoiem. Learning without forgetting. *IEEE transactions on pattern analysis and machine intelligence*, 40(12):2935–2947, 2017.
- [19] Hanul Shin, Jung Kwon Lee, Jaehong Kim, and Jiwon Kim. Continual learning with deep generative replay. In *Advances in Neural Information Processing Systems*, pages 2990–2999, 2017.
- [20] Mark Bishop Ring. Continual learning in reinforcement environments. *PhD thesis, University of Texas at Austin*, 1994.
- [21] Sebastian Thrun and Tom M Mitchell. Lifelong robot learning. *Robotics and autonomous systems*, 15(1-2):25–46, 1995.
- [22] Michael McCloskey and Neal J Cohen. Catastrophic interference in connectionist networks: The sequential learning problem. In *Psychology of learning and motivation*, volume 24, pages 109–165. Elsevier, 1989.
- [23] Roger Ratcliff. Connectionist models of recognition memory: constraints imposed by learning and forgetting functions. *Psychological review*, 97(2):285, 1990.
- [24] Haoxuan Qu, Hossein Rahmani, Li Xu, Bryan Williams, and Jun Liu. Recent advances of continual learning in computer vision: An overview. *arXiv preprint arXiv:2109.11369*, 2021.
- [25] Zhizhong Li and Derek Hoiem. Learning without forgetting. *IEEE transactions on pattern analysis and machine intelligence*, 40(12):2935–2947, 2017.
- [26] Prithviraj Dhar, Rajat Vikram Singh, Kuan-Chuan Peng, Ziyang Wu, and Rama Chellappa. Learning without memorizing. In *Proceedings of the IEEE/CVF Conference on Computer Vision and Pattern Recognition*, pages 5138–5146, 2019.
- [27] James Kirkpatrick, Razvan Pascanu, Neil Rabinowitz, Joel Veness, Guillaume Desjardins, Andrei A Rusu, Kieran Milan, John Quan, Tiago Ramalho, Agnieszka Grabska-Barwinska, et al. Overcoming catastrophic forgetting in neural networks. *Proceedings of the National Academy of Sciences of the United States of America*, 114(13):3521–3526, 2017.
- [28] F Zenke, B Poole, and S Ganguli. Continual learning through synaptic intelligence. *Proceedings of machine learning research*, 70:3987–3995, 2017.

- [29] Rahaf Aljundi, Francesca Babiloni, Mohamed Elhoseiny, Marcus Rohrbach, and Tinne Tuytelaars. Memory aware synapses: Learning what (not) to forget. In *Proceedings of the European Conference on Computer Vision (ECCV)*, pages 139–154, 2018.
- [30] Gobinda Saha, Isha Garg, and Kaushik Roy. Gradient projection memory for continual learning. In *International Conference on Learning Representations (ICLR)*, 2020.
- [31] Esra Ergün and Behçet Uğur Töreyn. Continual learning with sparse progressive neural networks. *2020 28th Signal Processing and Communications Applications Conference (SIU)*, pages 1–4, 2020.
- [32] Andrei A Rusu, Neil C Rabinowitz, Guillaume Desjardins, Hubert Soyer, James Kirkpatrick, Koray Kavukcuoglu, Razvan Pascanu, and Raia Hadsell. Progressive neural networks. *arXiv preprint arXiv:1606.04671*, 2016.
- [33] Sylvestre-Alvise Rebuffi, Alexander Kolesnikov, Georg Sperl, and Christoph H Lampert. icarl: Incremental classifier and representation learning. In *Proceedings of the IEEE conference on Computer Vision and Pattern Recognition*, pages 2001–2010, 2017.
- [34] David Lopez-Paz and Marc’Aurelio Ranzato. Gradient episodic memory for continual learning. *Advances in Neural Information Processing Systems (NIPS)*, 30, 2017.
- [35] Anthony Robins. Catastrophic forgetting, rehearsal and pseudorehearsal. *Connection Science*, 7(2):123–146, 1995.
- [36] Matthew Riemer, Ignacio Cases, Robert Ajemian, Miao Liu, Irina Rish, Yuhai Tu, , and Gerald Tesauro. Learning to learn without forgetting by maximizing transfer and minimizing interference. In *International Conference on Learning Representations (ICLR)*, 2019.
- [37] Arslan Chaudhry, Naeemullah Khan, Puneet Dokania, and Philip Torr. Continual learning in low-rank orthogonal subspaces. *Advances in Neural Information Processing Systems (NIPS)*, 33:9900–9911, 2020.
- [38] Ian J Goodfellow, Jonathon Shlens, and Christian Szegedy. Explaining and harnessing adversarial examples. *arXiv preprint arXiv:1412.6572*, 2014.
- [39] Aleksander Madry, Aleksandar Makelov, Ludwig Schmidt, Dimitris Tsipras, and Adrian Vladu. Towards deep learning models resistant to adversarial attacks. *arXiv preprint arXiv:1706.06083*, 2017.
- [40] Nicholas Carlini and David Wagner. Towards evaluating the robustness of neural networks. In *2017 IEEE Symposium on Security and Privacy (SP)*, pages 39–57. IEEE, 2017.
- [41] Gido M van de Ven and Andreas S Tolias. Three scenarios for continual learning. *arXiv*, pages arXiv–1904, 2019.
- [42] Yann LeCun, Corinna Cortes, and CJ Burges. Mnist handwritten digit database. 2010.
- [43] Nicolas Y Masse, Gregory D Grant, and David J Freedman. Alleviating catastrophic forgetting using context-dependent gating and synaptic stabilization. *Proceedings of the National Academy of Sciences*, 115(44):E10467–E10475, 2018.
- [44] Jonas Rauber, Roland Zimmermann, Matthias Bethge, and Wieland Brendel. Foolbox native: Fast adversarial attacks to benchmark the robustness of machine learning models in pytorch, tensorflow, and jax. *Journal of Open Source Software*, 5(53):2607, 2020.